Coordination of Cu^+ Ions to Zeolite Frameworks Strongly Enhances Their Ability To Bind NO_2. An ab Initio Density Functional Study

Luis Rodriguez-Santiago,[†] Marek Sierka,[‡] Vicenç Branchadell,[†] Mariona Sodupe,[†] and Joachim Sauer*,[‡]

Contribution from the Departament de Química, Universitat Autònoma de Barcelona, Edifici Cn, 08193 Bellaterra, Spain, and Max-Planck-Gesellschaft, Arbeitsgruppe Quantenchemie an der Humboldt-Universität, D-10117 Berlin, Germany

Received September 11, 1997. Revised Manuscript Received December 5, 1997

Abstract: Comparison is made of the interaction of NO_2 with Cu^+ ions in the gas phase and inside zeolites using density functional theory (B3LYP functional). The zeolite is represented by a tritetrahedra model embedded in the periodic structure of zeolite ZSM-5 and by a free space cluster model. Both models yield virtually the same results. Cu^+ is coordinated to two oxygen atoms of the zeolite framework only. For the complexes with NO_2, several minima and transition structures on the potential energy surfaces are localized. The naked Cu^+ ion preferentially binds NO_2 in the η^1-O trans mode, while in zeolites the Cu^+ site binds NO_2 in a $^2\eta$-O,O coordination. For the $^2\eta$-O,O structure the binding is three to four times stronger in the zeolite (43 kcal/mol) than in the gas phase which is due to a three-body zeolite framework—Cu^+ ion—NO_2 interaction. d^{10}−s^1d^9 promotion leads to a more favorable orbital interaction between Cu^+ and NO_2 in the $^2A''$ state and, due to reduced repulsion, to a stronger electrostatic interaction between Cu^+ and the zeolite framework.

1. Introduction

Transition metal cations show catalytic activity in different systems ranging from heterogeneous over homogeneous to biological. In recent years, it became possible to study the reactivity of naked (noncoordinated) transition metal cations.[1] Despite a fascinating chemistry revealed by these studies, catalytic activity could be observed in exceptional cases only, see, e.g., refs 2 and 3 An example is the role that Cu^+ ions play in the catalytic decomposition of NO_x—a mixture of NO and NO_2 of obvious environmental significance. Cu-exchanged zeolites, in particular Cu−ZSM-5, show a high and sustained activity.[4] Many studies reached the conclusion that the Cu^+ ion is in the core of the active sites of these catalysts.[5−8] In contrast, Schwarz and co-workers did not find any catalytic activity when investigating the [Cu^+, N, O] system in the gas phase.[9] This highlights the important role that ligands play in activating transition metal cations.

Some activation of Cu^+ and other transition metal ions by ligands has been observed before. The second water ligand was found to bind more strongly than the first one,[10] in contrast to alkaline metal ions, for which the energies for adding the next ligand are steadily decreasing when adding an increasing number of ligands. Confirmation came from ab initio calculations[11−13] which also provided the explanation:[12] “The unique feature of transition metal ions is their ability to reduce metal−ligand repulsion by sdσ hybridization. Since sdσ hybridization reduces the charge density along the σ axis, the second ligand binding energy can be larger than the first, because both ligands benefit from reduced repulsion while sharing the energetic cost of hybridization.” We will show below that the much stronger activation of Cu^+ ions by zeolite frameworks has a similar origin.

We study the interaction of NO_2 with Cu^+ ions in the gas phase and in zeolites. We localize several stationary points on the potential energy surfaces by ab initio methods employing density functional theory (DFT). We find a dramatic increase of the binding energy of NO_2 on the Cu^+ ion inside the zeolite compared with the naked Cu^+ ion. For a realistic description of this effect it is vital to have a valid model of the active site. In agreement with previous theoretical studies[14,15] we find that the Cu^+ ion is coordinated to two lattice oxygen atoms of the zeolite framework only, in contrast to the Cu^{2+} ion which prefers a higher coordination. Two is an unusually low coordination number for Cu^+, but it is confirmed by EXAFS studies on activated Cu-exchanged zeolites.[16,17] Our description includes

---

* Corresponding author: Humboldt Universität, Arbeitsgruppe Quantenchemie, Sitz: Jägerstrasse 10-11, D-10117 Berlin. E-mail: js@qc.ag-berlin.mpg.de.

[†] Universitat Autònoma de Barcelona.

[‡] Humboldt-Universität.

[1] Eller, K.; Schwarz, H. *Chem. Rev. (Washington, D.C.)* **1991**, *91*, 1121.

[2] Wesendrup, R.; Schröder, D.; Schwarz, H. *Angew. Chem., Int. Ed. Engl.* **1994**, *33*, 1174.

[3] Pavlov, M.; Blomberg, M. R. A.; Siegbahn, P. E. M.; Wesendrup, R.; Heinemann, C.; Schwarz, H. *J. Phys. Chem. A* **1997**, *101*, 1567.

[4] Shelef, M. *Chem. Rev. (Washington, D.C.)* **1995**, *95*, 209.

[5] Iwamoto, M.; Yahiro, H.; Tanda, K.; Mizuno, N.; Mine, Y.; Kagawa, S. *J. Phys. Chem.* **1991**, *95*, 3727.

[6] Li, Y.; Hall, W. K. *J. Catal.* **1991**, *129*, 202.

[7] Spoto, G.; Zecchina, A.; Bordiga, S.; Ricchiardi, G.; Martra, G.; Leofanti, G.; Petrini, G. *Appl. Catal. B: Environmental* **1994**, *3*, 151.

[8] Wichterlová, B.; Dědeček, J.; Sobalík, Z.; Vondrová, A.; Klier, K. *J. Catal.* **1997**, *169*, 194.

[9] Sülzle, D.; Schwarz, H.; Moock, K. H.; Terlouw, J. K. *Int. J. Mass Spectrom. Ion Proc.* **1991**, *108*, 269.

[10] Magnera, T. F.; David, D. E.; Stuhlik, D.; Orth, R. G.; Jonkman, H. T.; J. Michl *J. Am. Chem. Soc.* **1989**, *111*, 5036.

[11] Bauschlicher, C. W. J.; Langhoff, S. R.; Partridge, H. In *Organometallic Ion Chemistry*; Freiser, B. S., Ed.; Kluwer Academic Press: 1996; p 47.

[12] Bauschlicher, C. W. J.; Langhoff, S. R.; Partridge, H. *J. Chem. Phys.* **1991**, *94*, 2068.

[13] Rosi, M.; Bauschlicher, C. W. *J. Chem. Phys.* **1989**, *90*, 7264.

[14] Trout, B. L.; Chakraborty, A. K.; Bell, A. T. *J. Phys. Chem.* **1996**, *100*, 17582.

[15] Blint, R. J. *J. Phys. Chem.* **1996**, *100*, 19518.

S0002-7863(97)03196-X CCC: $15.00

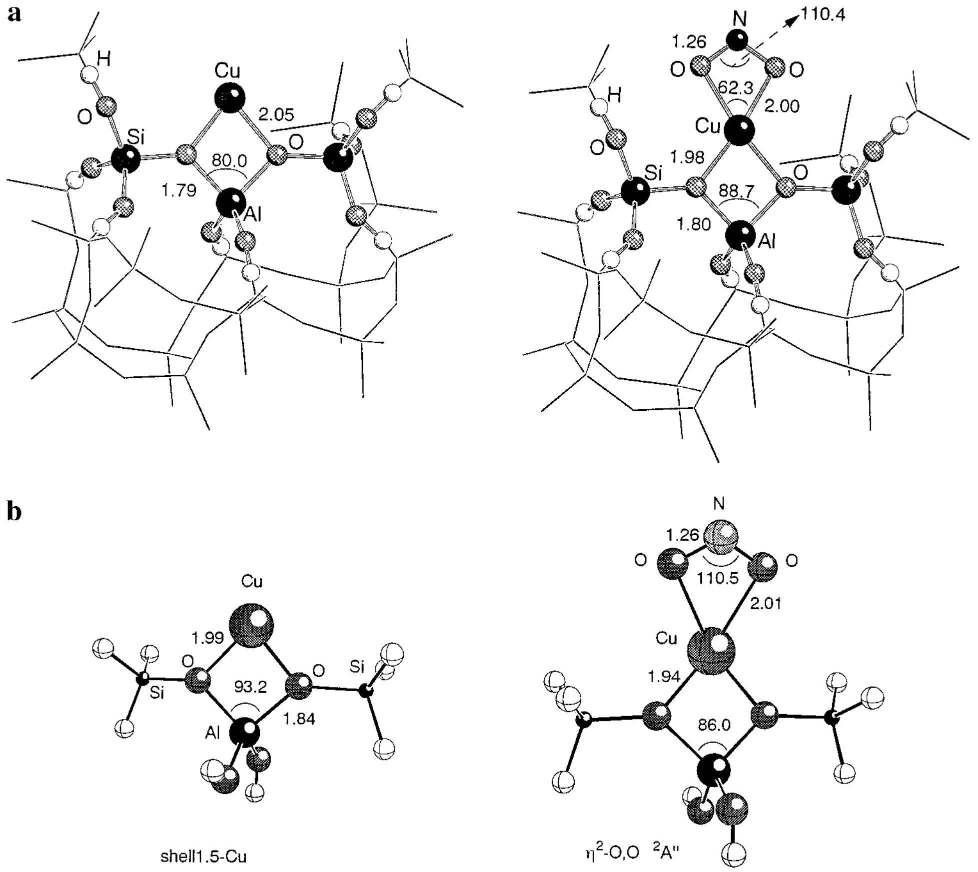

Figure 1. Predicted structures for the Cu^+ site in zeolites (left) and for its complex with NO_2 (right): (a) tritetrahedra model embedded into the periodic ZSM-5 structure and (b) zeolite framework represented by the shell-1.5 model.

the full periodic structure of the MFI framework (MFI is the common code for the framework type of ZSM-5 catalysts) for which we adopt the shell-model ion pair potential. We then determine the local structure of the Cu^+ site by embedding a model consisting of three tetrahedra (Figure 1a) into the periodic MFI structure and treat it quantum mechanically. We use for this purpose a recently developed combined quantum mechanics/interatomic potential approach (QM-pot).[18,19] We finally show that a virtually identical structure of the active site is obtained when using a nonembedded cluster model consisting of a central AlO_4^- tetrahedron and two neighbored SiO_4 tetrahedra (Figure 1b). This model, shell-1.5, proved successful in previous studies[20,21] and is used for the majority of structure predictions of the complexes of NO_2 with Cu^+ in zeolites. We finally show that the effect of the zeolite framework as ligand is special. The increase of the binding energy predicted for the zeolite is by far larger than that predicted for Cu^+ with two water molecules as ligands, even if we simulate the spatial arrangement of the two oxygen binding sites of zeolite frameworks by constraining the two water ligands to a bent configuration.

There is an increasing number of experimental and theoretical studies of the direct catalytic decomposition and the selective catalytic reduction of NO_x. This is not the place to give a complete account, nor it is our aim to study the whole mechanism. We focus here on NO_2, which is of interest not only as a pollutant itself but also as the product of the catalytic oxidation of NO.[22] Moreover, among several proposed mechanisms for the NO direct decomposition, the formation of the $ZCu{\cdot}NO_2$ complex has been suggested by several authors.[7,23,24] It can react with NO to form the $ZCu(NO_2)NO$ intermediate which decomposes into molecular nitrogen and oxygen.

Among the computational studies devoted to the problem[14,15,25−32] two are of particular relevance to our study. The DFT study of Yokomichi et al. compares the binding of NO to the naked Cu^+ ion and to the $[(HO)_2Al(OH)_2]^-Cu^+$ model for the Cu^+ site in zeolites.[30] They find enhanced binding although by far not as dramatic as found for NO_2 in the present study. They explain the effect by destabilization of d-orbitals due to interactions with the oxygen atoms of the zeolite skeleton. As

---

(16) Lamberti, C.; Bordiga, S.; Salvalaggio, M.; Spoto, G.; Zecchina, A.; Geobaldo, F.; Vlaic, G.; Bellatreccia, M. *J. Phys. Chem. B* **1997**, *101*, 344.

(17) Yamashita, H.; Matsuoka, M.; Tsuji, K.; Shioya, Y.; Anpo, M.; Che, M. *J. Phys. Chem.* **1996**, *100*, 397.

(18) Eichler, U.; Kölmel, C.; Sauer, J. *J. Comput. Chem.* **1996**, *18*, 463.

(19) Brändle, M.; Sauer, J. *J. Mol. Catal. A: Chem.* **1997**, *119*, 19.

(20) Haase, F.; Sauer, J. *J. Am. Chem. Soc.* **1995**, *117*, 3780.

(21) Krossner, M.; Sauer, J. *J. Phys. Chem.* **1996**, *100*, 6199.

(22) Shelef, M.; Montreuil, C. N.; Jen, H. W. *Catal. Lett.* **1994**, *26*, 277.

(23) Valyon, J.; Hall, W. K. *J. Catal.* **1993**, *143*, 520.

(24) Giamello, E.; Murphy, D.; Magnacca, G.; Morterra, C.; Shioya, Y.; Nomura, T.; Anpo, M. *J. Catal.* **1992**, *136*, 510.

(25) Hass, C.; Schneider, W. F. *J. Phys. Chem.* **1996**, *100*, 9292.

(26) Schneider, W. F.; Hass, K. C.; Ramprasad, R.; Adams, J. B. *J. Phys. Chem.* **1996**, *100*, 6032.

(27) Schneider, W. F.; Hass, K. C.; Ramprasad, R.; Adams, J. B. *J. Phys. Chem.* **1997**, *101*, 4353.

(28) Trout, B. L.; Chakraborty, A. K.; Bell, A. T. *J. Phys. Chem.* **1996**, *100*, 4173.

(29) Yokomichi, Y.; Ohtsuka, H.; Tabata, T.; Okada, O.; Yokoi, Y.; Ishikawa, H.; Yamaguchi, R.; Matsui, H.; Tachibana, A.; Yamabe, T. *Catal. Today* **1995**, *23*, 431.

(30) Yokomichi, Y.; Yamabe, T.; Ohtsuka, H.; Kakumoto, T. *J. Phys. Chem.* **1996**, *100*, 14424.

(31) Ramprasad, R.; Schneider, W. F.; Hass, K. C.; Adams, J. B. *J. Phys. Chem.* **1997**, *101*, 1940.

(32) Brand, H. V.; Redondo, A.; Hay, P. J. *J. Phys. Chem. B* **1997**, *101*, 7691.

part of their comprehensive analysis of possible intermediates in the NO_x decomposition process, Trout et al. study several isomers of the complex of NO_2 with a model of the Cu^+ ion in ZSM-5.[14] Their and our results for the structures and binding energies are remarkably similar, although there are some differences in the method used and the model adopted. Trout et al. use the local density approximation (LDA) and a different basis set. Their cluster model has the central AlO_4 tetrahedron surrounded by four SiO_4 tetrahedra, and the terminating OH groups are fixed at observed atomic positions.

2. Details of Calculations

DFT (density functional theory) calculations have been performed using the B3LYP functional which proved successful for a broad class of problems including transition metals[3,33−35] and which is a major improvement compared to LDA. The following basis sets optimized by Ahlrichs and co-workers have been adopted:[36] Cu − double-ζ augmented with a p function (exponent 0.155 065), i.e., [8s,6p,3d]; NO_2 − triple-ζ; zeolite models − triple-ζ on oxygen and double-ζ on all other atoms. Polarization functions with exponents 0.35, 0.30, 1.2, 1.0, and 0.8 are added to all Si, Al, O, N, and H atoms, respectively. DFT calculations are made using the TURBODFT code.[37] The coupled cluster CCSD(T) calculations follow in all details the description in ref 35 and use the GAUSSIAN code.[38]

Our calculations on the $Cu^+(H_2O)$ and $Cu^+(H_2O)_2$ complexes yield 43.8 and 44.6 kcal/mol for the binding of the first and second water ligand, respectively—slightly larger values than computed with the MCPF method by Bauschlicher et al. (40.5 and 41.3 kcal/mol)[12] or than inferred from experiments by Mangera et al. (35 ± 3 and 39 ± 3 kcal/mol).[10] We correctly reproduce the increased binding energy for the second ligand.

For describing the periodic zeolite structure both in the combined QM-pot approach and in the pure potential function energy minimizations the shell-model ion pair potential[39] is used. The combined QM-pot calculations make use of the TURBODFT[37] and the GULP[40] codes in the quantum and the shell-model ion pair potential part, respectively. The parameters for the ions of the anionic zeolite framework have been found by a fit to DFT data obtained with the same basis set as used here.[41] The parameters for Cu^+ are taken from ref 42. The parameters used are summarized in the Supporting Information.

3. Results and Discussion

3.1. Structure of the Cu^+ Site. First we performed a lattice energy minimization using the shell-model ion pair potential alone to determine the structure of the Cu^+ site in a periodic ZSM-5 environment. One Al atom per unit cell was substituted into the T12 position of the orthorhombic structure of MFI (96 TO_2 formula units, hence the Si/Al ratio is 95).[43] This position was also considered before,[14] and there is no reason to believe that the results will critically depend on the substitution site. It was found that the relative energies differ by no more than 5 kcal/mol when substituting Al in any of the 24 different sites. The T12 site was found only about 2.5 kcal/mol above the minimum energy substitution site. The lattice energy minimization was made in P1 symmetry and resulted in a monoclinic structure. The Cu^+ ion is found coordinated to two lattice oxygen atoms only. Even if the optimization was started with structures in which the Cu^+ ion was inside a five-membered ring the same 2-fold coordinated structure was found. Our observations are slightly at variance with the report of Sayle et al.[44] A more comprehensive simulation of a large variety of different Cu sites in ZSM-5 by a shell-model potential with parameters slightly different from ours also yielded dicoordinated Cu^+ sites, but the majority of Cu^+ sites had a larger coordination number. Note that the simulations of Sayle et al. also allowed OH^- species to coordinate to the Cu^+ ion.

Next we defined a tritetrahedra cluster (T3), $[(HO)_3SiO\text{-}Al(OH)_2OSi(OH)_3]^-$, around the Cu^+ site (Figure 1a), and a structure refinement was made using the combined QM-pot approach. The 2-fold coordination remained unchanged, and the $Cu^+\cdots Al$ and $Cu^+\cdots O$ distances changed to 2.8 and 2.05 Å, respectively. Trout et al. also found a 2-fold coordinated structure with slightly shorter bond distances. The $Al\cdots O$ distance was 2.4 Å, and two slightly different $Cu^+\cdots O$ bond distances of 1.95 and 1.86 Å were obtained. Hartree−Fock calculations on cluster models[15] also yield a 2-fold coordination of Cu^+ with $Cu^+\cdots O$ distances of 2.10 and 2.16 Å. These results are in agreement with the experimental structure information available. From $^{27}Al-^{65}Cu$ SEDOR NMR experiments on Cu−ZSM5 a Cu−Al distance of 2.3 ± 0.2 Å has been inferred.[45] The EXAFS experiments of Yamashita et al.[17] and Lamberti et al.[16] yield Cu−O distances of 1.94 and 2.00 Å, respectively. Other EXAFS and XANES data imply a coordination number of 2.1 and a mean Cu−O distance of 1.94 Å.[46,47]

Figure 1b shows the structure of the CuZ site obtained by DFT calculations when the zeolite is represented by the shell-1.5 model. The binding energy of Cu^+ to the shell-1.5 model is 160 kcal/mol. This model is OH terminated at the central Al atom, but H-terminated at the Si atoms. The tri-tetrahedra model adopted in the embedded cluster calculation is OH terminated on both the Al and the Si atoms. There is good agreement between this free cluster optimization and the embedded cluster calculations. Embedding has two effects. It constraints the relaxation of the cluster atoms (since they "feel" that they are part of the zeolite framework) and it adds long-range interactions. Comparison of parts a and b of Figure 1 shows that this has little effect on the coordination type and on the strength of the interaction. The $Cu^+\cdots O$ distances shrink by 2−3% only. We conclude that the shell-1.5 model without embedding provides a reasonable first information on the effect of coordinating the Cu^+ ion to the MFI framework.

---

[33] Bauschlicher, C. W.; Ricca, A.; Partridge, H.; Langhoff, S. R. In *Recent Advances in Density Functional Theory, Part II*; Chong, D. P., Ed.; World Scientific Publishing Company: Singapore, 1997.

[34] Holthausen, M. C.; Heineman, C.; Cornehl, H. H.; Koch, W.; Schwarz, H. *J. Chem. Phys.* **1995**, *102*, 4931.

[35] Rodriguez-Santiago, L.; Sodupe, M.; Branchadell, V. *J. Chem. Phys.* **1996**, *105*, 9966.

[36] Schäfer, A.; Horn, H.; Ahlrichs, R. *J. Chem. Phys.* **1992**, *97*, 2571.

[37] Treutler, O.; Ahlrichs, R. *J. Chem. Phys.* **1995**, *102*, 346.

[38] Head-Gordon, M.; Gill, P. M. W.; Wong, M. W.; Foresman, J. B.; Johnson, B. G.; Schlegel, H. B.; Robb, M. A.; Replogle, E. S.; Gomperts, R.; Andres, J. L.; Raghavachari, K.; Binkley, J. S.; Gonzalez, C.; Martin, R. L.; Fox, D. J.; Defrees, D. J.; Baker, J.; Stewart, J. J. P.; Pople, J. A. *GAUSSIAN 92*; Gaussian, Inc.: Pittsburgh, PA, 1992.

[39] Dick, B. G. J.; Overhauser, A. W. *Phys. Rev.* **1958**, *112*, 90.

[40] Gale, J. D. *J. Chem. Soc., Faraday Trans.* **1997**, *93*, 629.

[41] Sierka, M.; Sauer, J. *Faraday Discuss.* **1997**, *106*, 41.

[42] Sayle, D. C.; Perrin, M. A.; Nortier, P.; Catlow, C. R. A. *J. Chem. Soc., Chem. Commun.* **1995**, 945.

[43] van Koningsveld, H.; Jansen, J. C.; Bekkum, H. v. *Zeolites* **1990**, *10*, 235.

[44] Sayle, D. C.; Catlow, C. R. A.; Gale, J. D.; Perrin, M. A.; Nortier, P. *J. Phys. Chem.* **1997**, *101*, 3331.

[45] Hu, S.; Reimer, J. A.; Bell, A. T. *J. Phys. Chem.* **1997**, *101*, 1869.

[46] Liu, D. J.; Robota, H. J. *Appl. Catal. B* **1994**, *4*, 155.

[47] Liu, D.-J.; Robota, H. J. In *Reduction of Nitrogen Oxide Emissions*; ACS Symposium Series, Vol. 587 Ozkan, U.S., Agarwal, S. K., Marcelin, G., Eds.; American Chemical Society: Washington, DC, 1995; p 147.

[48] Ehrhardt, C.; Ahlrichs, R. *Theor. Chim. Acta* **1985**, *68*, 231.

Table 1. Binding Energies of NO_2 (kcal/mol), Relative Energies w.r.t. the Most Stable Structure Are Given in Parentheses

		$[Cu{\cdot}NO_2]^+$ this work			$ZCu{\cdot}NO_2$ this work	$ZCu{\cdot}NO_2$ ref 14
structure		CCSD(T)//B3LYP	B3LYP		B3LYP	LSD
η^1−O trans		19.6 (0.0)	26.4 (0.0)		30.3 (12.4)	
η^1−O cis		17.1 (2.4)	24.3 (2.1)		30.0 (12.7)	12.2 (30.4)
η^1−N		7.7 (11.9)	16.4 (10.0)		25.1 (17.6)	26.8 (15.8)
η^2−N,O		7.1 (12.5)	16.4 (10.0)		35.8 (6.9)	
η^2−O,O	$^2A_1$	10.4 (9.1)	14.0 (12.4)	$^2A'$	10.7(32.0)	
	$^2B_2$		10.5 (15.9)	$^2A''$	42.7 (0.0)	42.6 (0.0)

Table 2. Results of Mulliken Population Analysis and, in Parentheses, a Population Analysis Based on Occupation Numbers (Ref 48)

			charge		spin density		metal orbital population		
			Cu	NO_2	Cu	NO_2	s	p	d
	ZCu		0.57				6.34	12.24	9.85
			(1.02)						
η^2−O,O	Cu^+NO_2	$^2A_1$	0.83	0.18	0.13	0.87	6.14	12.07	9.96
			(0.99)	(0.01)	(0.05)	(0.93)			
	$ZCuNO_2$	$^2A'$	0.72	−0.25	0.53	0.38	6.47	12.33	9.47
			(1.13)	(−0.30)	(0.75)	(0.34)			
	Cu^+NO_2	$^2B_2$	0.87	0.13	0.40	0.60	6.42	12.16	9.55
			(0.82)	(0.18)	(0.40)	(0.60)			
	$(H_2O)_2Cu^+NO_2$	$^2A''$	0.70	−0.13	0.58	0.35	6.54	12.37	9.37
	$ZCuNO_2$	$^2A''$	0.68	−0.32	0.63	0.20	6.57	12.42	9.33
			(0.91)	(−0.35)	(0.62)	(0.20)			
η^2−N,O	Cu^+NO_2	$^2A'$	0.85	0.15	0.23	0.77	6.23	12.08	9.83
			(0.87)	(0.13)	(0.35)	(0.65)			
	$ZCuNO_2$		0.67	−0.26	0.50	0.36	6.50	12.41	9.43
			(0.83)	(−0.27)	(0.49)	(0.37)			

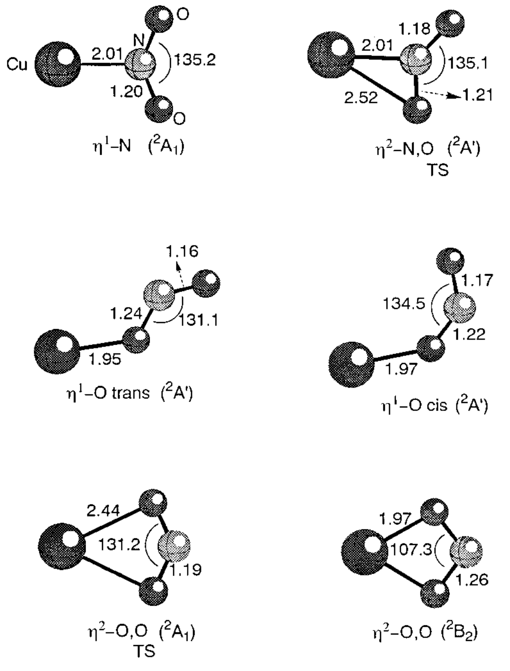

Figure 2. Predicted structures of different isomers and electronic states of the Cu^+-NO_2 gas-phase complex.

3.2. Structure and Stability of Cu^+NO_2 Gas-Phase Complexes. Figure 2 and Table 1 show the DFT(B3LYP) results for the different structure isomers of NO_2 interacting with Cu^+ in the gas phase and for the stabilization energies. Different coordination modes have been found: the bidentate η^2-O,O and η^2-N,O coordinations and the monodentate η^1-O (cis and trans) and η^1-N coordinations. Only the η^1-O and η^1-N modes are minima on the ground-state potential energy surface. The most stable isomer is η^1-O (trans), with η^1-O (cis) being only 2.1 kcal/mol higher in energy. The η^2-O,O structure ($^2A_1$ state) is the transition state connecting the two equivalent η^1-O cis isomers, while the η^2-N,O one corresponds to the η^1−O (trans) → η^1−N isomerization. The η^1-N structure is a very shallow minimum with almost the same energy as the η^2-N,O transition structure. Comparison is made with CCSD(T) single point results. The binding energies are reduced in all cases, but the relative stability of the local minima is maintained and the transition structures remain above the minima they connect.

The bonding in the ground state ($^2A'$ and $^2A_1$) is mainly noncovalent and arises from the interaction of the $^1S(d^{10})$ state of Cu^+ and the $^2A_1$ ground state of NO_2. The relative stability of the different isomers can be understood in terms of metal−ligand repulsion and electrostatic attraction. Table 2 shows for the η^2-O,O and η^2-N,O transition structures that—in agreement with this view—the metal orbital population stays close to $d^{10}s^0$, the unpaired electron remains localized on NO_2, and the positive excess charge remains on Cu. Consistently, the structure of the NO_2 fragment in the complex is very similar to that of the $^2A_1$ state of free NO_2 at the same level of calculation (Table 3).

The $^2B_2$ state of the η^2-O,O coordination is a minimum on an excited potential energy surface. It can be viewed as the interaction of the $^1S(d^{10})$ state of Cu^+ with the $^2B_2$ state of NO_2. The geometric structure of the NO_2 fragment in this state is very similar to that of the $^2B_2$ state of free NO_2 (Table 3). The left-hand side of Figure 3 shows the most relevant orbitals involved in the bond between Cu^+ and NO_2. The orbital occupation is given for the $^2A_1$ ground state of NO_2. In the $^2B_2$ excited state the $4b_2$ orbital is singly occupied, while the $6a_1$ orbital is doubly occupied. This opens the possibility for an electron donation from the doubly occupied $6a_1$ orbital of

---

(49) Morino, Y.; Tanimoto, M.; Saito, S.; Hirota, E.; Awata, R.; Tanaka, T. *J. Mol. Spectrosc.* **1983**, *98*, 331.

(50) Kaldor, U. *Chem. Phys. Lett.* **1991**, *185*, 131.

(51) Ervin, K. M.; Ho, J.; Lineberger, W. C. *J. Phys. Chem.* **1988**, *92*, 5405.

(52) Hughes, B. M.; Lifschitz, C.; Tiernan, T. O. *J. Chem. Phys.* **1973**, *59*, 3162.

Table 3. Bond Distance (Å) Bond Angle (deg), and Electron Affinity (EA, eV) for NO_2[e]

		r(NO)	∠ONO	EA
NO_2	$^2A_1$	1.194	134.2	
	obsd	(1.194)[a]	(133.9)[a]	
	$^2B_2$	1.254	101.7	
	calcd	(1.270)[b]	(100.6)[b]	
NO_2^-	$^1A_1$	1.264	116.0	1.85
	obsd	(1.25 ± 0.02)[c]	(117.5 ± 2.0)[c]	(2.28)[d]

[a] Reference 49. [b] CCSD method, ref 50. [c] Reference 51. [d] Reference 52. [e] Observed results or other computed results in parentheses.

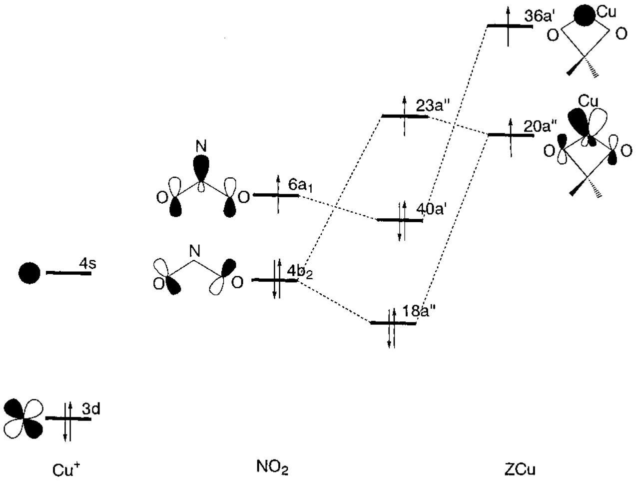

Figure 3. Diagram of the most important orbitals involved in the formation of the bond between the Cu$^+$ site and NO_2.

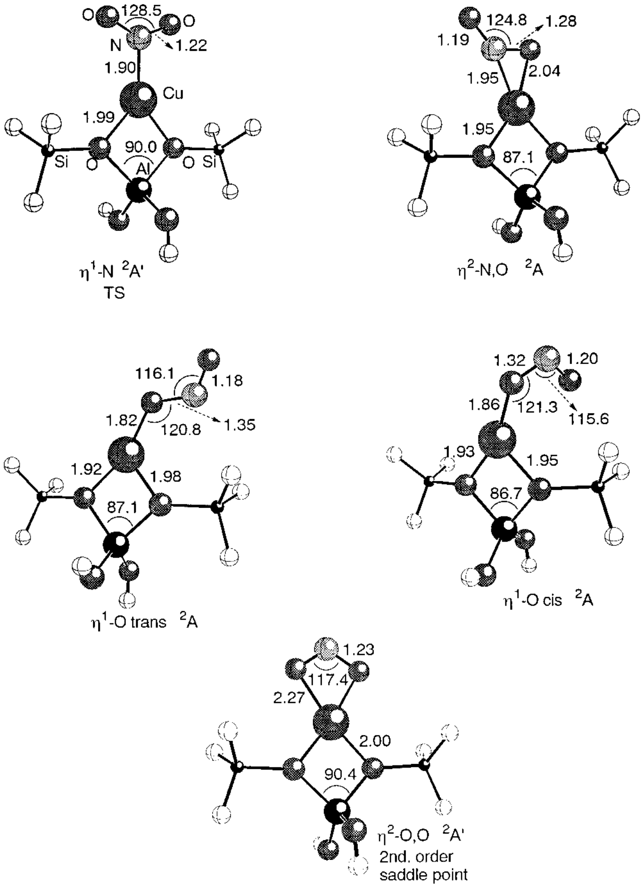

Figure 4. Predicted structures of different isomers of the $ZCuNO_2$ complex ($^2A'$ and ^2A states). The zeolite framework is replaced by the shell-1.5 model in the calculations.

NO_2 to the 4s orbital of Cu and some back-donation from the 3d orbital on Cu to the singly occupied $4b_2$ orbital on NO_2. In effect, there is some 3d−4s promotion (d-population about 9.5, cf. Table 2), and this state can also be described as bonding between Cu$^+$ (d^9s^1) and the $^2A_1$ state of NO_2.

3.3. Complexes of NO_2 with Cu$^+$ in Zeolites. Figure 4 shows the structures and Table 1 the binding energies for the complexes of NO_2 with the Cu$^+$ attached to the zeolite model (CuZ). When coordinated to the zeolite framework, the Cu$^+$ ion interacts more strongly with NO_2. In general, the distances between Cu and NO_2 are shorter, and the binding energies are larger. Major changes on the topology of the potential energy surfaces occur. The η^1-O minimum structures (cis and trans) and the η^2-O,O transition structure ($^2A_1 - {}^2A'$ states) show the least changes. In the former the binding becomes stronger, while the latter is further destabilized. For the η^2-N,O structure the binding is significantly increased and it becomes a local minimum now, while it was a transition structure in the gas-phase complex. The η^1-N coordination is also stabilized but not as much as the η^2-N,O structure. In the zeolite complex it becomes a transition structure connecting the two symmetrical η^2-N,O minima, while it was a local minimum in the gas-phase complex.

A particular striking case is the $^2B_2$ state of the η^2-O,O complex. In the gas phase it was least binding and an excited state. In the zeolite complex we also find the corresponding state, $^2A''$. However, now it is the most stable one and represents the global minimum. It is four times more stable than the $^2B_2$ state and three times more stable than the $^2A_1$ state of the η^2-O,O complex in the gas phase. Compared with the most strongly bound gas-phase complex (η^1-O trans) the binding energy increases by 62%. To confirm this unusually strong binding effect, we have investigated the η^2-O,O complex of NO_2 by the embedded cluster method. NO_2 was interacting with the quantum part only, but relaxation of the positions of the nuclei of the embedded model was constraint by forces from all the atoms of the periodic zeolite framework. Figure 1a shows the structure found which is virtually identical with that of the complex involving the shell-1.5 model shown in Figure 1b. The binding energy, 42.0 kcal/mol, differs by less than 1 kcal/mol from the result in Table 1. It remains to be seen if this agreement between a free space cluster model which does not represent any specific site and a specific model (T12 site in ZSM-5) persists if additional sites of the MFI framework or different frameworks are considered. If so, there would be an interesting implication: The activation of Cu$^+$ ions by zeolite frameworks for NO_2 binding is not connected with a particular site in a particular framework. If, e.g., ZSM-5 proves to be a particular efficient Cu-containing catalysts, this may have other reasons than different intrinsic properties of the different Cu$^+$[(≡SiO)$_2$Al(O-)$_2$]$^-$ sites.

Before, Yokomichi et al. found that Cu$^+$ attached to a $(OH)_2Al(OH)_2^-$ model of the zeolite framework binds NO more strongly than the naked Cu$^+$ ion.[30] The increase was from 38 to 51 kcal/mol—not as large as found here for NO_2.

To analyze the dramatic effect of binding energy increase, we look at the relevant orbitals of NO_2 and ZCu shown in Figure 3. Note that the orbital occupancies shown apply to only one of the different situations discussed below. Z in ZCu stands for the shell-1.5 zeolite model. In the ground state of ZCu the 20a″ orbital is the HOMO of Cu$^+$ and doubly occupied. This orbital is mainly the d_{xy} orbital of Cu$^+$ mixed with the $4p_y$ orbital to polarize away from Z$^-$ to reduce repulsion. Thus, the side opposite to the zeolite surface is a high electron density region,

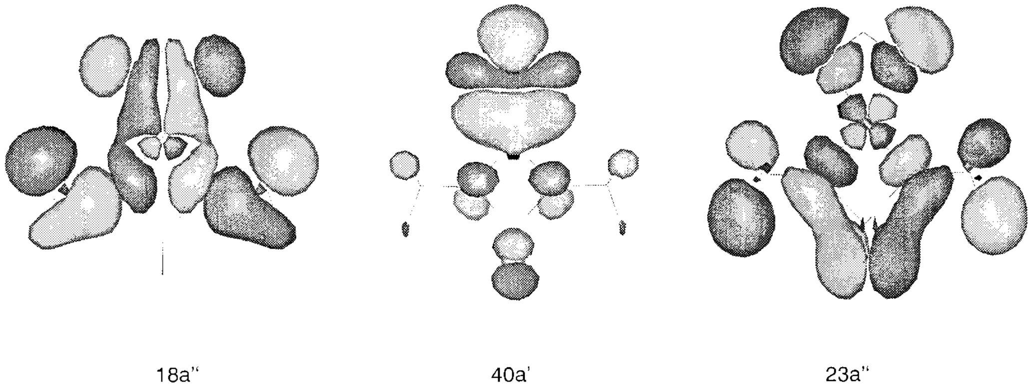

Figure 5. Representation of the 18a″, 40a′, and 23a″ orbitals of the $^2\eta$-O,O isomer of $ZCuNO_2$ in its electronic ground state.

and there is an increased repulsion for the NO_2 ligand approaching the Cu^+ ion on the zeolite wall. The repulsion with all ligands can be reduced by 3d−4s promotion. In the ZCu model this promotion becomes much easier (1.9 eV) than in the naked Cu^+ ion (2.6 eV). We have already seen that the interaction of the naked Cu^+ ion in its d^{10} ground state with NO_2 in its excited $^2B_2$ state results in a 3d−4s promotion. Since this promotion is also facilitated by an increased electrostatic attraction between the Cu^+ ion and the zeolite wall, there is a mutual enhancement. Due to the reduced repulsion between Cu^+ and Z^- in the $^2A''$ state of $ZCuNO_2$, the $Cu^+\cdots O$(zeolite) distances shrink by 0.05 Å on NO_2 bonding, both for the embedded T3 model (Figure 1a) and the nonembedded shell-1.5 model (Figure 1b). This leads to a gain in the electrostatic energy between Cu^+ and Z^-.

We can also start our consideration from the "opposite" situation, NO_2 in its $^2A_1$ ground state and a fully promoted Cu^+ state (d^9s^1). Figure 3 shows the orbital occupancies for this situation. The 36 a′ orbital of the ZCu system which was the LUMO in the d^{10} ground state is now singly occupied. This orbital is mainly the 4s orbital of Cu^+. It interacts with the $6a_1$ orbital of NO_2 which is singly occupied in the $^2A_1$ ground state to give a doubly occupied a′ orbital (40a′, Figure 5). The singly occupied 20a″ orbital (d_{xy}) on Cu^+ interacts with the doubly occupied $4b_2$ orbital of NO_2 to yield the singly occupied 23a″ orbital above and the doubly occupied 18a″ orbital below the 40 a′ orbital (Figure 5). Since this three-electron interaction is connected with some donation from the $4b_2$ orbital of NO_2 to the 3d orbital on Cu (20a″) and some back-donation from the 4s orbital of Cu^+ to the $6a_1$ orbital of NO_2, the NO_2 gets partially excited and the d^9s^1 state gets less s and more d character. This view is supported by the observation that the structure of the $CuNO_2$ fragment in the $^2A''$ state of the ZCuNO2 complex is very similar to that of the $^2B_2$ state of the η^2-O,O Cu^+NO_2 gas-phase complex (see Figures 1b and 2).

The picture of the bonding is further confirmed by the population analysis given in Table 2. The d occupation on Cu in $ZCuNO_2$ is 9.33—a decrease by 0.52 electrons compared to ZCu. In the gas-phase complex, in which 3d−4s promotion is not enhanced by the Cu^+−zeolite interaction, the 3d population is closer to the d^{10} state, 9.55. Moreover, the Mulliken spin density indicates that the unpaired electron is mainly located on the metal ion since the most important contribution to the singly occupied orbital 23a″ comes from the Cu d_{xy} orbital (20a″) of ZCu.

The $^2A'$ electronic state of the η^2-O,O $ZCuNO_2$ complex lies 32 kcal/mol above the $^2A''$ ground state. In this case the 40a′ orbital is the open shell orbital and the 23a″ orbital that is antibonding between ZCu and NO_2 is doubly occupied (Figure 3). Since the Cu contribution to the former is mainly 4s and to the latter mainly 3d (Figure 3), the 3d population in the $^2A'$ state is larger than in $^2A''$, while the 4s population is smaller (Table 2). Figure 3 also shows that the $(18a'')^2(40a')^1(23a'')^2$ occupation corresponds to the orbital occupation in the $^2A_1$ ground state of NO_2. Hence, in the $^2A'$ state of η^2-O,O $ZCuNO_2$ the structure of the $CuNO_2$ fragment is closer to the $^2A_1$ state of gas-phase Cu^+NO_2 than to the $^2B_2$ state (Figure 2 and Table 3). Frequency calculations on the $^2A'$ state show that this stationary point is a second-order saddle point. The movement associated with one of the imaginary frequencies leads to the η^1-O structure (cis), while the other one corresponds to the NO_2 rotation. Since this structure has a very high energy and rotation of NO_2 is not expected to decrease the energy significantly, we have not studied this electronic state further.

For the η^2-N,O coordination the binding energy of the $ZCuNO_2$ complex is twice as large as in the gas phase. The reason is that for this coordination mode the $6a_1$ orbital of NO_2 has the proper local symmetry to interact with the HOMO of ZCu (20a″). The resulting three-electron interaction becomes a more stabilizing two-electron interaction when an electron is promoted from 3d (20a″) to 4s (36a′). This 3d−4s promotion on the Cu atom is much larger for ZCu than for Cu for the reasons discussed above. Note that due to reduced repulsion on 3d−4s promotion the $Cu^+\cdots O$ distance shrinks from 1.99 Å in ZCu (Figure 1b) to 1.95 Å in the $ZCuNO_2$ complex (Figure 4). The orbital occupation data of Table 2 support this view. The d population on Cu decreases from 9.85 and 9.83 in ZCu and η^2-N,O Cu^+NO_2, respectively, to 9.43 in η^2-N,O $ZCuNO_2$. The population analysis (Table 2) shows that in Cu^+NO_2 the spin density is mainly located in the NO_2 fragment, while in $ZCuNO_2$ half of the spin is on Cu.

From the above considerations follows that the effect of a largely increased bond strength with Cu^+ in a zeolite is coupled to the presence of a singly occupied orbital available for bonding in the energy region where the Cu orbitals are found. When binding water instead of NO_2 to the CuZ complex, the binding energy calculated for the shell-1.5 model (27 kcal/mol—a similar value has been reported before[15]) decreases compared to the Cu^+OH_2 gas-phase complex energy (43.8 kcal/mol).

To understand if the effect found is specific for zeolites as ligands of Cu^+ or may be also present with other oxygen ligands we have made additional calculations on the $Cu^+(H_2O)_2NO_2$ system (η^2-O,O coordination, $^2B_2$ state). Figure 6 shows the optimized structure. The orbital interactions are the same as in the $^2A''$ state of $ZCuNO_2$, and the structure of the $CuNO_2$ fragment is almost identical (cf. Figures 1 and 6). However, the binding energy computed with respect to the linear equilibrium structure of $Cu^+(H_2O)_2$ is 4.7 kcal/mol only. If it is calculated with the bent structure of $Cu^+(H_2O)_2$ as reference,

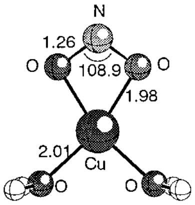

Figure 6. Predicted structure of the $(H_2O)_2Cu^+NO_2$ complex.

i.e., with all structure parameters the same as in the $(H_2O)_2$-Cu^+NO_2 complex, a value of 23.5 kcal/mol is obtained—larger than for the naked Cu^+ ion but still far from that obtained for Cu^+ in zeolites (42.7 kcal/mol). Promotion from d^{10} to d^9s^1 is found as costly (2.6 eV) as for the free Cu^+ ion.

We conclude that half of the activating effect that the zeolite framework has on Cu^+ ions is that it holds the oxygen ligands in the proper position. About the other half is due to the stronger bonding between the negatively charged zeolite surface and the positively charged Cu^+ ion in the presence of NO_2. When 3d−4s promotion reduces repulsion, the zeolite-Cu distance can shrink and there is a gain in electrostatic energy. In contrast, the Cu^+-OH_2 distance is larger in the $(H_2O)_2Cu^+NO_2$ complex (2.02 Å) than in the linear $Cu^+(H_2O)_2$ system (1.98 Å). The Cu^+-OH_2 distance optimized for the bent structure of the $Cu^+(H_2O)_2$ system (O−Cu−O angle fixed to its optimum value in the $(H_2O)_2Cu^+NO_2$ complex) is 2.05 Å. This indicates that with respect to the bent structure as reference there is some reduction of repulsion, but the gain in electrostatic energy (ion−dipole) is not as large as in the $ZCuNO_2$-system (ion-pair interaction).

This has implications for selecting models of the Cu^+ site in zeolites. Although the local structure of the active site of the zeolite and the bonding mechanism can be reasonably well represented by the most simple Cu^+−water models,[25,26,31,32] the unusually strong binding energy of NO_2 (this work) and NO (ref 30) changes significantly from such simple models to the more realistic ones studied in this and previous work (e.g. refs 14,15,28−30).

4. Conclusion

The coordination of Cu^+ to the zeolite framework results in a substantially stronger bonding of NO_2 and in different preferred coordination modes compared to the gas-phase complex between Cu^+ and NO_2. This effect is due to $d^{10}-d^9s^1$ promotion which reduces repulsion with all ligands of Cu^+. As a result orbital interactions between Cu^+ and NO_2 become more favorable and electrostatic interactions between Cu^+ and the negatively charged zeolite wall more attractive. Hence we observe a cooperative (three-body) effect in the system $zeolite^-Cu^+NO_2$ which strengthens both the NO_2-Cu^+ and the Cu^+-$zeolite^-$ interactions.

Acknowledgment. Most calculations for this study have been made when L.R. was at Humboldt-University. Financial support for his stay from the Spanish Minister of Education and Science is gratefully acknowledged. This work has also been supported by the "Fonds der Chemischen Industrie" and by the "Deutsche Forschungsgemeinschaft".

JA973196K